MOLECULAR AND CELLULAR BIOLOGY, Jan. 2006, p. 718–726 Vol. 26, No. 2
0270-7306/06/$08.00+0 doi:10.1128/MCB.26.2.718–726.2006

Oligo-Astheno-Teratozoospermia in Mice Lacking RA175/TSLC1/SynCAM/IGSF4A, a Cell Adhesion Molecule in the Immunoglobulin Superfamily

Eriko Fujita,[1] Yoriko Kouroku,[1] Satomi Ozeki,[1] Yuko Tanabe,[1] Yoshiro Toyama,[2] Mamiko Maekawa,[2] Naosuke Kojima,[3] Haruki Senoo,[3] Kiyotaka Toshimori,[2] and Takashi Momoi[1]*

Division of Differentiation and Development, Department of Inherited Metabolic Disorder, National Institute of Neuroscience, NCNP, Oawahigashi-machi 4-1-1, Kodaira, Tokyo 187-8502,[1] Department of Anatomy and Developmental Biology, Graduate School of Medicine, Chiba University, Inohana 1-8-1, Chiba, Chiba 260-8670,[2] and Department of Cell Biology and Histology, Akita University School of Medicine, 1-1-1, Hondo, Akita 010-8543,[3] Japan

Received 11 August 2005/Returned for modification 26 September 2005/Accepted 24 October 2005

RA175/TSLC1/SynCAM/IGSF4A (RA175), a member of the immunoglobulin superfamily with Ca^{2+}-independent homophilic *trans*-cell adhesion activity, participates in synaptic and epithelial cell junctions. To clarify the biological function of RA175, we disrupted the mouse *Igsf4a* (*Ra175*/*Tslc1*/*SynCam*/*Igsf4a Ra175*) gene. Male mice lacking both alleles of *Ra175* (*Ra175*$^{-/-}$) were infertile and showed oligo-astheno-teratozoospermia; almost no mature motile spermatozoa were found in the epididymis. Heterozygous males and females and homozygous null females were fertile and had no overt developmental defects. RA175 was mainly expressed on the cell junction of spermatocytes, elongating and elongated spermatids (steps 9 to 15) in wild-type testes; the RA175 expression was restricted to the distal site (tail side) but not to the proximal site (head side) in elongated spermatids. In *Ra175*$^{-/-}$ testes, elongated and mature spermatids (steps 13 to 16) were almost undetectable; round spermatids were morphologically normal, but elongating spermatids (steps 9 to 12) failed to mature further and to translocate to the adluminal surface. The remaining elongating spermatids at improper positions were finally phagocytosed by Sertoli cells. Furthermore, undifferentiated and abnormal spermatids exfoliated into the tubular lumen from adluminal surfaces. Thus, RA175-based cell junction is necessary for retaining elongating spermatids in the invagination of Sertoli cells for their maturation and translocation to the adluminal surface for timely release.

RA175/TSLC1/SynCAM/IGSF4A (RA175) is a new member of the immunoglobulin superfamily that has three immunoglobulin domains in its extracellular region and EYFI, a type II PDZ (postsynaptic density 95/disk large/zonula occludens-1)-binding domain, in its C-terminal intracellular region and has Ca^{2+}-independent homophilic *trans*-cell adhesion activity (10). RA175 was at first isolated as one of the genes preferentially expressed during the neuronal differentiation of P19 mouse embryonal carcinoma (P19 EC) cells induced by retinoic acid (9, 21) and is localized in the mouse developing nervous system and epithelium of various organs (2, 10, 11, 29). In the nervous system, RA175 is designated the synaptic cell adhesion molecule (SynCAM) and has been suggested to be involved in the formation of functional synapses (2). The localization of RA175 also suggests its biological role in the migration of neurons and the fasciculation of axons (11). In the developing lung epithelium, RA175 is localized in the cell-adherent region of the basolateral membrane in the polarized cells lining the lumen (10). Defects in *IGSF4A/tumor suppressor gene in lung cancer 1* (*TSLC1*), an orthologue of mouse *Igsf4a* (*Ra175*), promote the metastasis of lung carcinoma cells (18). However, little is known about its real biological function during organ development. To clarify the biological function of RA175, we disrupted the murine *Ra175* gene. Male mice lacking both alleles of *Ra175* (*Ra175*$^{-/-}$) were infertile, whereas heterozygous males and females and homozygous null females were fertile and had no overt developmental defects.

The junctional complex formed near the base of Sertoli cells is composed of ectoplasmic specialization and tight, gap, and desmosome-like junctions, and it divides the microenvironment into the basal and adluminal compartments (8). Spermatogonia and early spermatocytes, which are located in the basal compartment, are in contact with the basement membrane and Sertoli cells, whereas differentiating spermatocytes and spermatids, which are located in the adluminal compartment, are in contact with only Sertoli cells and therefore receive nutrition, hormones, and local factors exclusively from Sertoli cells.

Various cell adhesion molecules have been shown to be involved in the cell junction during spermatogenesis (3, 15, 16, 19, 22, 23). Among these, nectins and junctional adhesion molecule C (Jam-C)/Jam-3 (Jam-C), members of the immunoglobulin superfamily, have been shown to play essential roles in spermatogenesis (3, 15, 23). Poliovirus receptor-related 2 (pvrl2)/nectin-2 (nectin-2) and pvrl3/nectin-3 (nectin-3) are localized on the elongated spermatid (steps 9 to 16) and Sertoli cells, respectively, and form actin-based Sertoli-spermatid junctions that are involved in the assembly of actin filaments in the ectoplasmic specialization (26). Jam-C is localized on the round and elongated spermatids and mediates polarization of

* Corresponding author. Mailing address: Division of Differentiation and Development, Department of Inherited Metabolic Disorder, National Institute of Neuroscience, NCNP, Ogawahigashi-machi 4-1-1, Kodaira, Tokyo 187-8502, Japan. Phone: 81-42-341-2711. Fax: 81-42-346-1778. E-mail: momoi@ncnp.go.jp.

the adhesion junction with Sertoli cells by associating with partitioning-defective-3 (PAR-3) (15). Homozygous null males of *Nectin-2*$^{-/-}$ and *Jam-C*$^{-/-}$ are infertile (3, 15, 23). *Nectin-2*$^{-/-}$ male mice show a random disorganization of the spermatozoan head and midpiece due to overall disorganization of cytoskeletal structure, but they have motile spermatozoa (3, 23). *Jam-C*$^{-/-}$ male mice have an almost complete lack of elongated spermatids as a result of a defect in the polarization of adhesion junctions on the round spermatids, and they fail to produce mature sperm cells (15).

Here we show that *Ra175*$^{-/-}$ male mice are also infertile but have different phenotypes from *Nectin-2*$^{-/-}$ and *Jam-C*$^{-/-}$ male mice. They are defective in spermiogenesis, fail to produce mature sperm cells, and have severe oligo-astheno-teratozoospermia (low sperm number, low motility, and abnormal sperm morphology). In addition, we discuss the biological role of RA175 in spermiogenesis and the relationship between RA175 and other cell adhesion molecules.

MATERIALS AND METHODS

In situ hybridization. The EcoRI fragment of *RA175* in the pGEM-T easy vector was subcloned into pBluescript SK(+) vectors in both the sense and anti-sense orientations as previously described (29). Digoxigenin (DIG)-labeled *RA175* RNA probes were transcribed from XhoI-cut constructs using T3 RNA polymerase (DIG RNA Labeling kit T3; Boehringer Mannheim, Mannheim, Germany) in vitro according to the manufacturer's instructions. Frozen sections (10 μm thick) of mouse embryos at 13 embryonic days (E13.5) and testes of 4-week-old mice were treated with proteinase K (1 μg/ml) at 37°C for 10 min, refixed in 4% paraformaldehyde, and hybridized overnight with the DIG-labeled RNA probes. Hybridized RNA was detected using alkaline phosphatase-conjugated anti-DIG according to the procedure described by Wilkinson (31).

Generation of *Ra175*$^{-/-}$ mice. A 12-kb mouse *Igsf4a* (Mouse Genome Informatics accession no. 1889272, *Ra175*) genomic DNA fragment was cloned from the mouse 129Sv/Ev bacterial artificial chromosome genomic library. This genomic fragment contains exon 1 (13). The clone starts from 8.1 kb upstream of exon 1 and ends 3.8 kb downstream of exon 1, with a sequence of 5′-AATCTC TTATGTATAAAGCTGAAATGTACCAGG-3′. One side of the *lacZ-neo* gene cassette was inserted 5 bp upstream of the start ATG codon on exon 1. The sequence that was replaced starts with 5′-CCGACATGGCGAGTGCTGTGCT GCCGAGCGGATCCCAGTGTGCGGCGG-3′. The other side of the *lacZ-neo* gene cassette was inserted 2.4 kb downstream of exon 1 inside intron 1. The sequence that was replaced ends with 5′-TAGGGCTTGCTAAGACTCTCTCT CAAACTGTATAC-3′. In this strategy, the *lacZ-neo* cassette replaced the coding region of exon 1 and part of intron 1. As a result, the original *Ra175* promoter drives the LacZ expression. Ten micrograms of the targeting vector was linearized by NotI and then transfected by electroporation of 129 SvEv embryonic stem (ES) cells. After selection in G418 antibiotic, 300 surviving colonies were expanded for PCR analysis to identify recombinant clones.

To identify the wild-type and targeted alleles, primer pairs 5′-TGGCCCCTT CTAAGAAATACCCTC-3′ and 5′-GATTTGTAGCGAGGGAATGAGATGA C-3′ at 2.3 kb downstream of exon 1 and 5′-CCCAATAAGTCTCATAGAAC TGATTGTC-3′ and 5′-TGCGAGGCCAGAGGCCACTTGTGTAGC-3′ primers at the 5′ end of the Neo cassette were used for PCR analysis, respectively. The PCR amplified the 1.8-kb fragment for wild-type allele and 1.6-kb fragments for targeted allele at 94°C for 20 s, 62°C for 60 s, and 72°C for 120 s for 35 cycles, and then 72°C for 10 min. The correctly targeted ES cell lines were microinjected into the C57BL/6J blastocysts, and the chimeras were then set up for mating with the C57BL/6J mice, and they gave germ line transmission of the mouse *Ra175lacZ* knock-in gene. We intercrossed heterozygous *Ra175* mice to produce homozygous *Ra175*$^{-/-}$ mice.

X-Gal staining of mouse testis. LacZ activity in *Ra175*$^{-/-}$ testes was detected by 5-bromo-4-chloro-3-indolyl-β-D-galactopyranoside (X-Gal) staining as previously described (25). Mouse testes 10 to 12 weeks after birth were embedded in freezing medium and frozen on dry ice. The embedded testes were sectioned at a 15 μm thickness at −15°C. Each section was transferred onto a silanized slide and allowed to dry and fixed in a fixing solution (0.2% glutaraldehyde, 2 mM $MgCl_2$, and 5 mM EGTA in phosphate-buffered saline [PBS]). After being washed three times in a washing solution (2 mM $MgCl_2$, 0.01% sodium deoxycholate, and 0.02% Nonidet P-40 in PBS), each section was stained in the X-Gal staining solution [1 mg/ml X-Gal, 5 mM $K_3Fe(CN)_6$, 5 mM $K_4Fe(CN)_6$, and 2 mM $MgCl_2$ in PBS] at 30°C overnight. After being stained, testes were washed and stored in PBS.

Sperm count and motility analysis. We placed cauda epididymides in 0.1 ml of motile buffer (120 mM NaCl, 5 mM KCl, 25 mM $NaHCO_3$, 1.2 mM KH_2PO_4, 1.2 mM $MgSO_4$, and 1.3 mM $CaCl_2$). We minced the tissue with scissors and incubated it at 37°C for 5 min to allow sperm dispersal. The supernatant was obtained as a sperm suspension, and the motility of sperm in the suspension was visually monitored under phase-contrast images (IM type; Olympus, Tokyo, Japan). After 25-fold and/or 50-fold dilution, the number of sperm in the 0.1-μl suspension was counted by using cell counter plates under the microscope.

Immunohistochemical staining. Antibodies against a peptide corresponding to the C-terminal region of RA175 were prepared as previously described (10) and were used for the immunostaining. Testes of 10- to 12-week-old *Ra175*$^{+/+}$ and *Ra175*$^{-/-}$ male mice were fixed in 4% paraformaldehyde in phosphate-buffered saline (PBS) at 4°C overnight and then soaked in 30% sucrose-PBS at 4°C overnight and embedded in optimal cutting temperature compound (Sakura Finetec. Co., Ltd., Tokyo, Japan) and frozen. Frozen sections (10 μm thick) were cut on a cryostat and attached to Matsunami adhesive silane-coated slides (Matsunami Glass Co., Osaka, Japan) and incubated with rabbit anti-RA175 in PBS containing 0.1% skim milk and 0.1% Triton X-100 at 4°C for 2 days as described previously (10). Anti-RA175 immunoreactivity was detected using anti-rabbit immunoglobulin G-Alexa Fluor 568 (Molecular Probes, Eugene, OR). Acrosome structure was detected using fluorescein isothiocyanate-conjugated peanut agglutinin (PNA) (J-Oilmills, Tokyo, Japan) staining in place of *p*-aminosalicylic acid staining. F-actin was detected using Alexa Flour 568-phalloidin (Molecular Probes). Nuclei were detected by Hoechst 33342 dye at 37°C for 15 min. The sperm tail was detected by Alexa Fluor 568 Mitotracker (Molecular Probes). Immunoreactivity was viewed using a confocal laser-scanning microscope (CSU-10; Yokogawa, Tokyo, Japan).

Conventional light microscopy. We fixed testes of male mice (10 to 12 weeks of age) in Bouin or 4% paraformaldehyde neutral buffer solution, embedded them in paraffin, and cut 8-μm sections on a microtome. We stained sections with hematoxylin and eosin by standard procedures.

Conventional transmission electron microscopy. Adult mice (12 to 16 weeks of age) were perfusion fixed through the left ventricle with 3% glutaraldehyde in HEPES buffer (10 mM HEPES ethansulfanic acid [Nacalai Tesque, Kyoto, Japan] containing 145 mM NaCl). Testes cut into small pieces were immersed in the same fixative for an additional 2 h. The samples were then postfixed in 1% OsO_4 for 1 h. After routinely dehydrated with graded ethanol series, the samples were embedded in Epon812 and the ultrathin sections were made on an ultramicrotome (Ulreacut E; Reihert-jung, Vienna, Austria). The thin sections were stained with uranyl acetate and lead citrate and observed with a JEM 1200 EX (JEOL, Tokyo, Japan) transmission electron microscope. One-micrometer semithin sections were stained with toluidine blue for light microscopy.

RESULTS

To make clear the relationship between the biological function of RA175 and organ development, we examined the expression of *Ra175* mRNA in mouse embryos. In situ hybridization showed that *Ra175* mRNA was expressed in the nervous tissues including brain, spinal cord, and dorsal root ganglia (Fig. 1A and B) as well as in various epithelia, including hair follicles (Fig. 1B and C), lung epithelium (Fig. 1D), esophagus epithelium (Fig. 1E), olfactory epithelium (Fig. 1F), and tongue epithelium (Fig. 1G) in mouse embryos at embryonic day 13.5 (E13.5). It was also expressed in testes 4 weeks after birth (Fig. 1H) in spermatocytes and spermatids.

To determine the biological function of RA175, we inactivated *Ra175* in mouse ES cells by replacing exon 1 of the *Ra175* gene with the *lacZ* reporter gene cassette (Fig. 2A). Cell lines that had undergone a targeting event were used to generate mice that transmitted the disrupted gene. These mice were mated to produce *Ra175*$^{+/-}$ mice. Intercrosses yielded offspring (~20 litters) that segregated with the expected Mendelian frequency: 41 wild type, 101 heterozygotes (*Ra175*$^{+/-}$), and 42 homozygotes (*Ra175*$^{-/-}$) by PCR analysis (Fig. 2B).

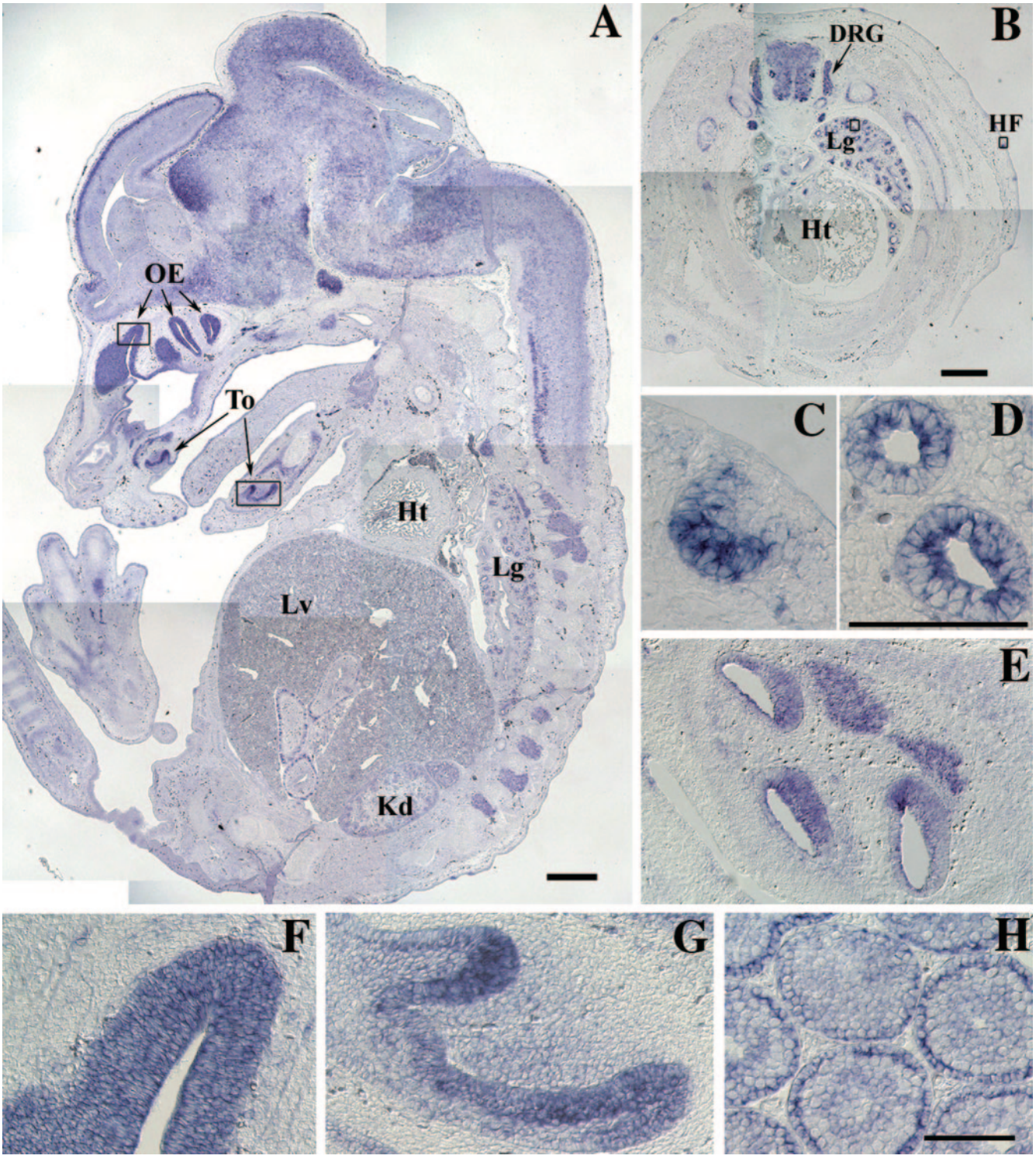

FIG. 1. In situ hybridization analysis of the expression of *Ra175* mRNA in mouse embryos and testes. Expression of the *Ra175* mRNA on the sagittal section (A) and transverse section of trunks (B) of mouse embryo at E13.5. (C to G) Magnification of the epithelium of each organ in the rectangular region in panels A and B. (C) Hair follicle; (D) lung; (E) esophagus; (F) olfactory epithelium; (G) tongues epithelium; (H) testis of the 4-week-old mouse. OE, olfactory epithelium; To, tongue; Lg, lung; Lv, liver; Kd, kidney; Ht, heart; DRG, dorsal root ganglia; HF, hair follicle. In addition to the nervous system including brain, spinal cord, and dorsal root ganglia, *Ra175* mRNA was detected in the various epithelium of the developing organs. Bars in panels A and B, 500 μm. Bars in panels C to H, 200 μm.

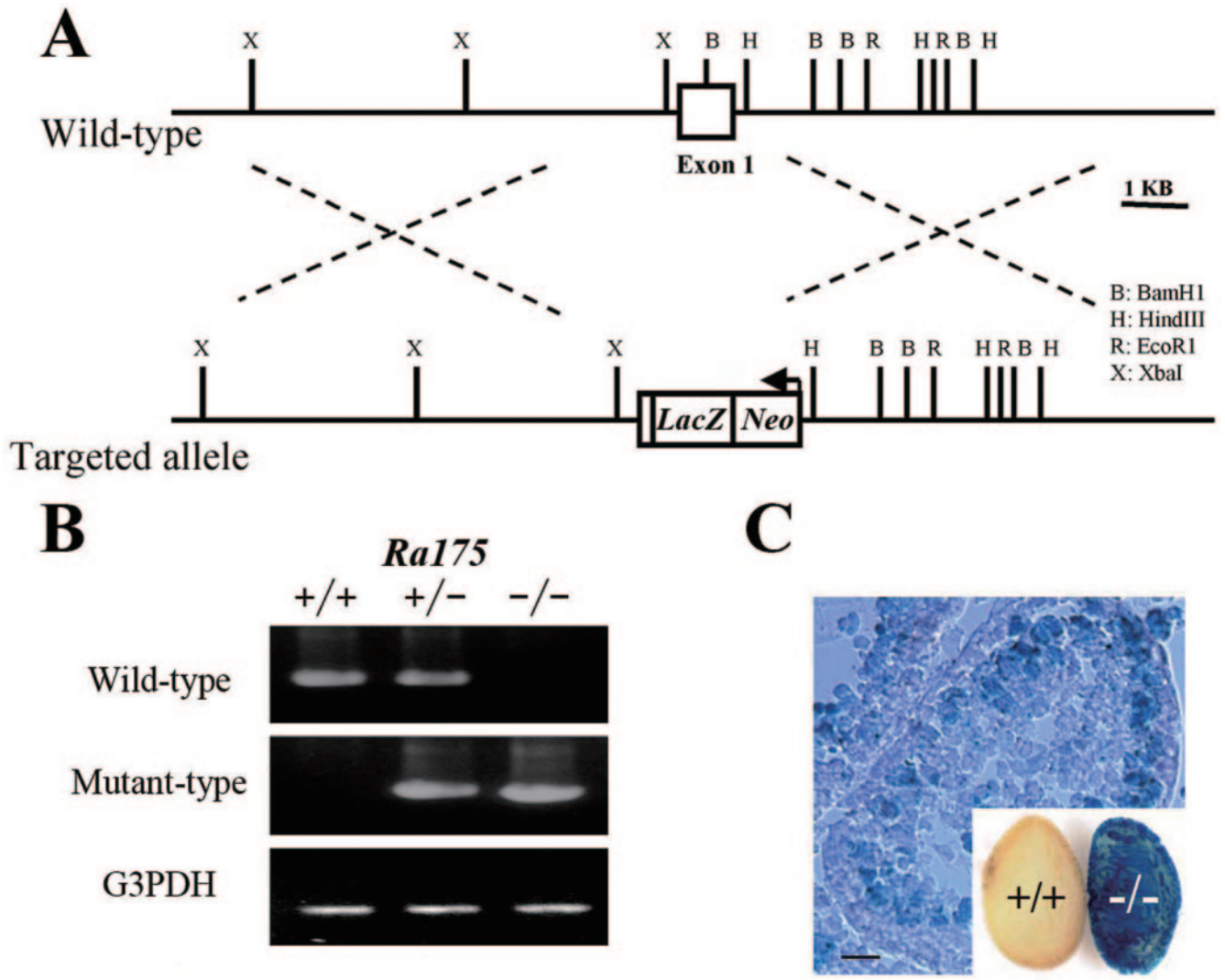

FIG. 2. Targeted disruption of the mouse *Ra175* gene. (A) Structure of the wild-type allele and the targeted allele. Exon 1 of the *Ra175* gene was replaced by *lacZ* and *neo* genes as described in Materials and Methods. (B) Genotype analysis of wild-type, heterozygote, and homozygote mice by PCR. (C) X-Gal staining of $Ra175^{+/+}$ and $Ra175^{-/-}$ testes. LacZ activity was detected in the germ cells including spermatocytes. Bar, 10 μm.

Male mice lacking both alleles of *Ra175* ($Ra175^{-/-}$) were infertile, while $Ra175^{+/-}$ males and females and $Ra175^{-/-}$ females were fertile. $Ra175^{-/-}$ mice had no overt developmental defects in the nervous tissues or other tissues except for in testes. Consistent with the finding of *Ra175* mRNA expression in the wild-type testes (Fig. 1H), LacZ activity was detected in the germ cells including spermatocytes in $Ra175^{-/-}$ testes but not in $Ra175^{+/+}$ testes (Fig. 2C).

The weight of $Ra175^{-/-}$ testes was about 15% lower than that in the wild-type ($Ra175^{+/+}$) animals. In severe cases, most spermatozoa were lost in the seminiferous tubules of the $Ra175^{-/-}$ mice, and only a small number remained (Fig. 3A). These remaining spermatozoa did not have motility (Fig. 3B). Thus, $Ra175^{-/-}$ males show oligo-asthenozoospermia (low sperm number and low motility).

A detailed histological analysis of seminiferous tubules from $Ra175^{-/-}$ mice clearly showed that in contrast with $Ra175^{+/+}$ (Fig. 4A and C), residual bodies and the midpieces of sperm

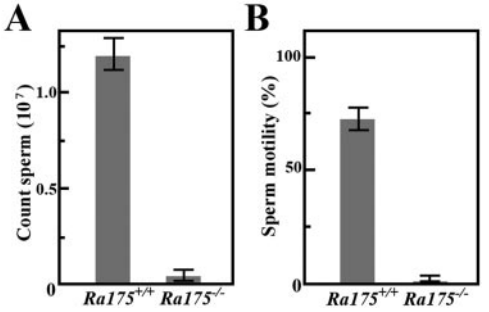

FIG. 3. Number of spermatozoa and the motility of $Ra175^{+/+}$ and $Ra175^{-/-}$ mice. The number of spermatozoa (A) from $Ra175^{+/+}$ and $Ra175^{-/-}$ mice and their motility (B). Normal and abnormal cells with nuclei were counted as spermatozoa. The value is the average of three experiments. $Ra175^{-/-}$ males show low sperm number and motility. Error bars indicate standard deviation. Statistical significance ($P < 0.05$) in each assay was assessed by Student's *t* test.

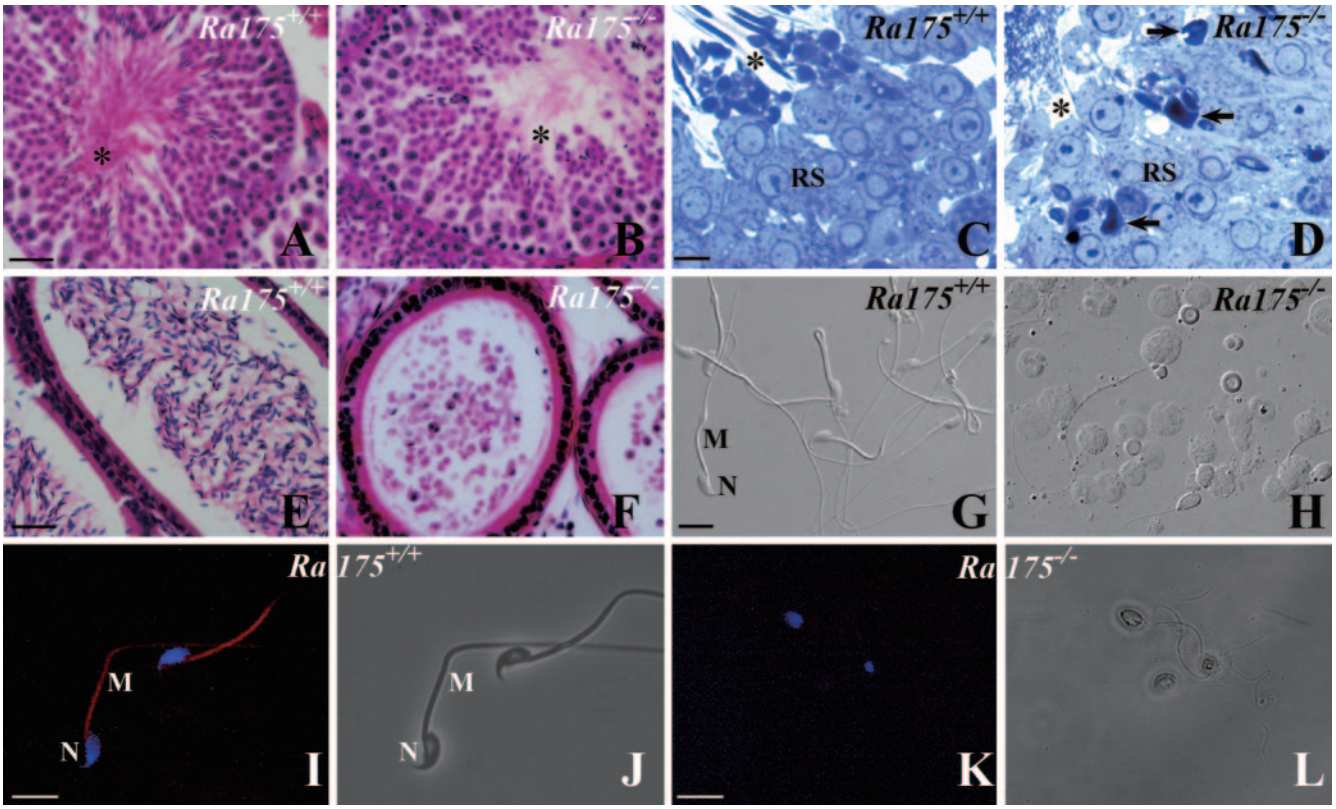

FIG. 4. Spermatogenesis at stage VIII and germ cells in the cauda epididymidis of *Ra175*$^{+/+}$ and *Ra175*$^{-/-}$. (A, C, E, G, I, and J) *Ra175*$^{+/+}$; (B, D, F, H, K, and L) *Ra175*$^{-/-}$; (A, B, E, and F) hematoxylin and eosin (HE) staining; (C and D) toluidine blue staining; (G and H) Nomarski images; (I and K) fluorescence images with Mitotracker staining for mitochondria (red) and Hoechst staining for the nucleus (blue); (J and L) bright-field images. Compared to normal spermatogenesis in *Ra175*$^{+/+}$ testes (A and C), spermatogenesis normally proceeds until the round spermatid stage (B and D), but abnormally shaped germ cells appear in elongating stages (B) in *Ra175*$^{-/-}$ testes. In contrast with *Ra175*$^{+/+}$ testes (A and C), the areas for the residual bodies and the thick portions of spermatid tails (mitochondrial regions indicated by asterisks) are almost absent in *Ra175*$^{-/-}$ testes (B and D). In contrast with *Ra175*$^{+/+}$ (E, G, I, and J), mature spermatozoa are not detected, but many exfoliated germ cells are detected in the cauda epididymal lumen of *Ra175*$^{-/-}$ (F, H, K, and L). Note that thick portions (mitochondrial regions) are absent in the exfoliated elongated spermatid tails in the *Ra175*$^{-/-}$ (H, K, and L). Thus, immature elongated spermatids in the *Ra175*$^{-/-}$ cauda epididymidis lacked mitochondrial region, which eventually leads to sterility. RS, round spermatids; M, middle piece; N, nucleus. Arrows indicate irregular nuclei. Bars in panels A, B, E, and F, 20 μm. Bars in panels C and D, 5 μm. Bars in panels G to L, 10 μm.

tails (asterisk) were almost not present in *Ra175*$^{-/-}$ testes (Fig. 4B and D). Round spermatids were morphologically normal, but elongated spermatids showed abnormally shaped heads in *Ra175*$^{-/-}$ testes, and they were not localized at the adluminal surface. Furthermore, very few morphologically mature elongated spermatids were detected in *Ra175*$^{-/-}$ testes (Fig. 4B and D). Thus, germ cells differentiated normally into the round spermatid stage but abnormally into the elongated spermatid stage.

Germ cells including round spermatids exfoliated at various stages of differentiation in *Ra175*$^{-/-}$ testes and were found in the lumen of the cauda epididymides (Fig. 4E to L). The remaining spermatozoa had irregularly shaped heads, abnormally arranged mitochondria (Fig. 4K and L), and erroneously attached flagella (unpublished observation) as well as round heads, probably due to the abnormal differentiation from round spermatids (Fig. 4H). Thus, *Ra175*$^{-/-}$ males showed oligo-astheno-teratozoospermia (low sperm number, low motility, and abnormal sperm morphology) leading to sterility.

We examined the localization of RA175 during spermiogenesis. The stage of spermatid differentiation is closely associated with changes in the acrosomal system. Localization of RA175

TABLE 1. Localization of RA175 during spermiogenesis classified by PNA and acrosomal structure[a]

Spermiogenesis stage (step)	PNA	RA175
Round spermatids (1 to 5)	+ (acrosomal granules)	±
Round spermatids (6 to 8)	+ (cap acrosome)	±
Elongating spermatid (9 to 12)	+ (flattened cap acrosomis)	+ (mostly distal site)
Elongated spermatid (13 to 15)	−	+ (only distal site)
Mature spermatid (16)	−	−

[a] The normal spermatid differentiation of the wild type are mainly classified into five groups by PNA staining and acrosomal structures as follows: (i) Round spermatids (steps 1 to 5); PNA-positive acrosomal granules and RA175-weakly positive. (ii) Round spermatid (steps 6 to 8); PNA-positive cap formation of acrosome and RA175-weakly positive. (iii) Elongating spermatid (steps 9 to 12); PNA-positive flattened cap formation of acrosome and RA175 is positive on the cell junction of the distal site and a few proximal head portion. (iv) Elongated spermatid (steps 13 to 15); PNA-negative and RA175 is positive on the cell junction of the distal site (tail side) but negative on the proximal site (head site). (v) Mature spermatid (step 16); RA175-negative, no residual bodies.

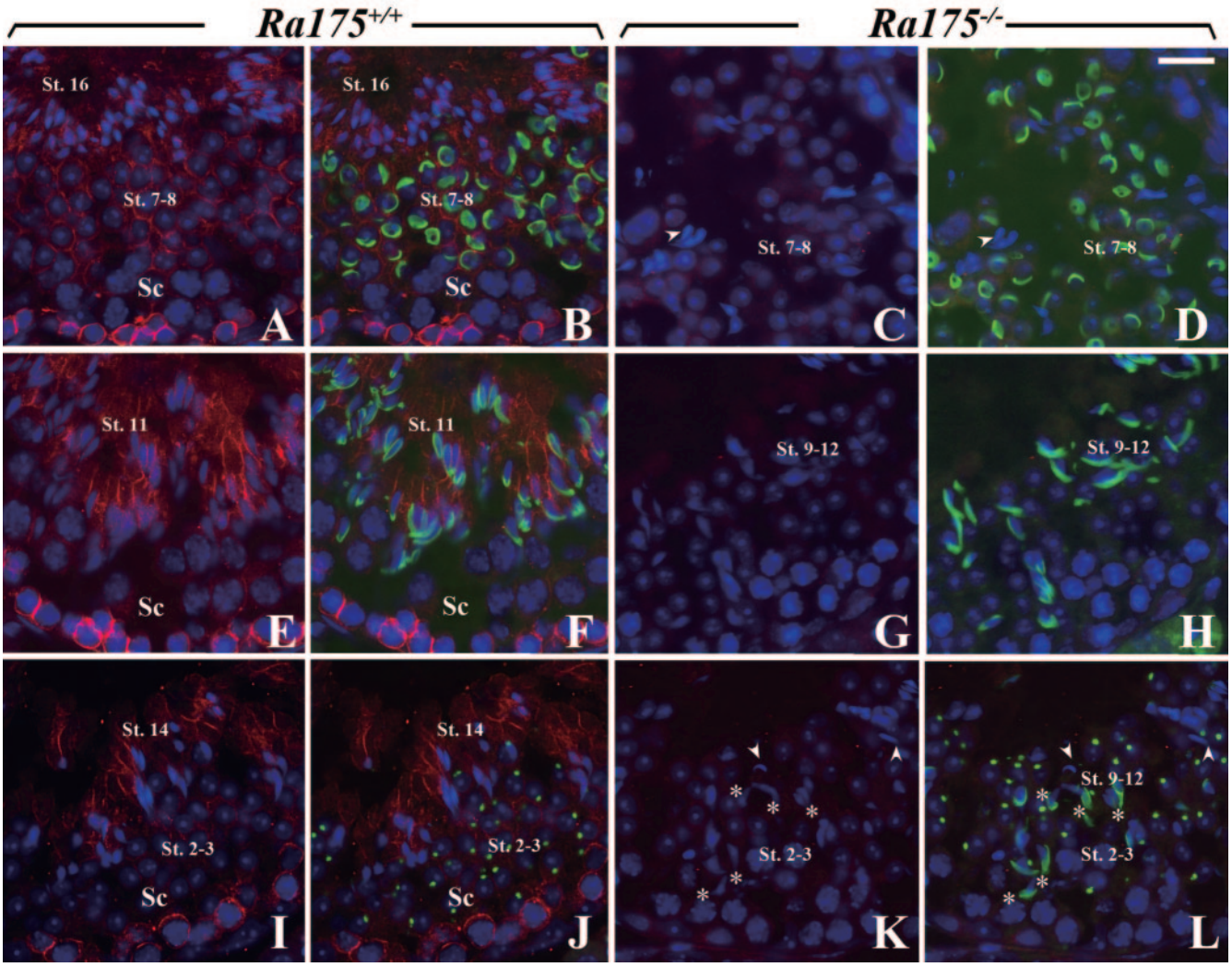

FIG. 5. Localization of RA175 during the differentiation from round to elongated spermatids in *Ra175*$^{+/+}$ and *Ra175*$^{-/-}$ testes. (A, B, E, F, I, and J) *Ra175*$^{+/+}$; (C, D, G, H, K, and L) *Ra175* $^{-/-}$. (A, C, E, G, I, and K) Merged images of spermatids stained with anti-RA175 (red) and Hoechst staining (blue). (B, D, F, H, J, and L) Merged images of spermatids stained with anti-RA175 (red), fluorescein isothiocyanate-conjugated PNA (green), and Hoechst staining (blue). (A to D) Stage VII; (E to H) stage XI; (I and J) stages II and III; (K and L) stages XII to II/III. Steps of the spermiogenesis of *Ra175*$^{-/-}$ testes were not exactly determined due to abnormal differentiation and lack of elongated spermatids. The differentiation of round to elongated spermatids was assessed by PNA staining (Table 1), which recognizes the acrosomal structure. Spermiogenesis normally occurs in *Ra175*$^{+/+}$ testes, whereas in *Ra175*$^{-/-}$ testes, PNA-positive elongating spermatids (steps 9 to 12; asterisks in K and L) appear but stay together with the PNA-positive round spermatid (steps 2 and 3; K and L), probably due to the translocation failure. Elongated spermatids (steps 13 to 15) were almost not detected in *Ra175*$^{-/-}$ testes (arrowheads in panels C, D, K, and L). St., step; Sc, spermatocytes. Bar, 20 μm.

during spermiogenesis (steps 1 to 16) could be mainly classified into five groups by peanut agglutinin (PNA) staining (Table 1), which recognizes the Golgi and acrosomal structures (15). In addition to the cell junctions between Sertoli cells and spermatocytes (Fig. 5A, B, E, F, I, and J), RA175 was strongly expressed in the cell junction of the elongating (step 11 in Fig. 5E and F) and elongated spermatids (step 14 in Fig. 5I and J) but weakly expressed on the round spermatids (steps 7 and 8 in Fig. 5A and B and steps 2 and 3 in Fig. 5I and J). In the elongating (steps 9 to 12) and elongated spermatid (steps 13 and 14), RA175 was mainly localized on the cell junctions of the distal site (Fig. 5E, F, I, and J) and tail side of elongated spermatids that faced to the lumen of tubules at stages XI to VI. After displacement of residual bodies, RA175 reactivity was remarkably reduced in the mature spermatids (step 16 in Fig. 5A and B).

PNA staining confirmed that acrosome formation of the round spermatid (steps 6 to 8) was not compromised in *Ra175*$^{-/-}$ testes (Fig. 5C and D). The elongating spermatids (steps 9 to 12) also appeared (Fig. 5G and H), but the elongated spermatids (PNA negative; steps 13 to 16) were hardly detected at the adluminal surface or other sites (arrowheads in Fig. 5C, D, K, and L). The elongating spermatids failed to proceed into further maturation steps and were not translocated to the adluminal surface. The remaining elongating spermatids (asterisks in Fig. 5K and L) decreased in their cell number but stayed together with the round spermatids (steps 1 to 5), which appeared in the same region (Fig. 5L).

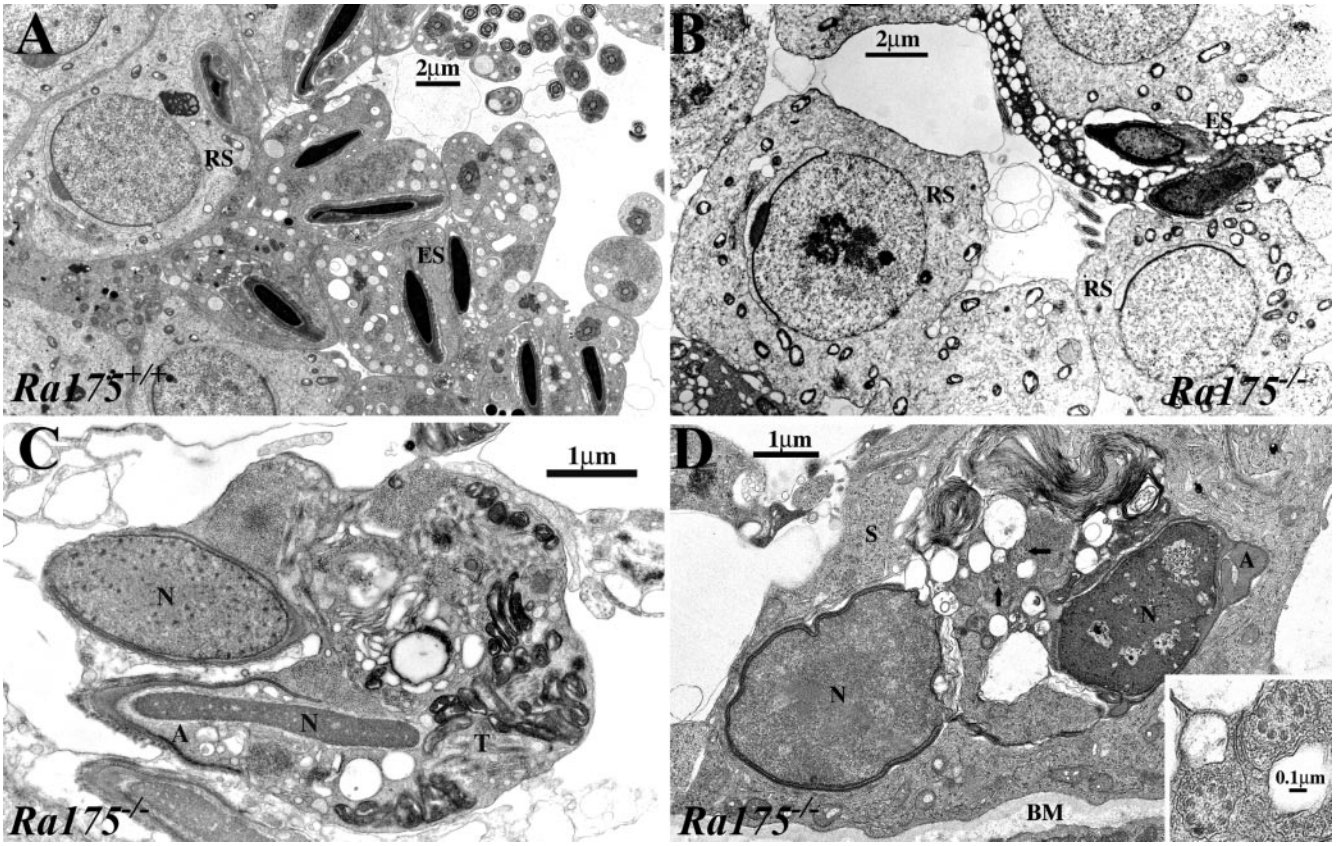

FIG. 6. Electron micrographs showing normal spermatogenesis in *Ra175*$^{+/+}$ testes and abnormal spermatogenesis in *Ra175*$^{-/-}$ testes. All germ cell images are taken from seminiferous tubules at around stage VIII. Compared to *Ra175*$^{+/+}$ (A), *Ra175*$^{-/-}$ germ cells (B) are capable of developing normally to round spermatid (RS) stage, whereas elongating spermatids start to degenerate and form irregular nuclei with incomplete condensation (ES in panel B). (C) Elongating spermatids are frequently formed as a symplast in which malformed sperm components are found; e.g., incompletely condensed nuclei (N), incompletely developed acrosome (A), and disorganized tail components (T). (D) Degenerated germ cells, which have ill-formed nuclei (N), acrosome (A), and axoneme (arrows), are readily phagocytosed by Sertoli cells. Inset, higher magnification of axoneme (arrowed area). BM, basement membrane.

Thus, the steps of the spermiogenesis were disturbed in *Ra175*$^{-/-}$ testes.

Electron microscopy analyses clarified that compared to the normal spermatogenesis in *Ra175*$^{+/+}$ testes (Fig. 6A), round spermatids developed normally and formed acrosomes, but the condensation of elongated spermatids was incomplete in *Ra175*$^{-/-}$ testes (Fig. 6B). Symplasts, which are formed by undivided elongating spermatids, were frequently formed, and they contained ill-formed sperm components such as incompletely condensed nuclei, abnormally formed acrosomes, and disorganized tail components (Fig. 6C). Interestingly, degenerated spermatids, which had ill-condensed nuclei, unusually shaped acrosomes, and disarranged tail components, were readily phagocytosed by Sertoli cells (Fig. 6D). Owing to this, the number of elongating spermatids was reduced, eventually leading to oligozoospermia. Thus, *Ra175*$^{-/-}$ spermatocytes could normally differentiate into the round spermatids but failed to differentiate into the elongated spermatids.

DISCUSSION

The phenotypic difference between *Ra175*$^{-/-}$ and *Rxrb*$^{-/-}$ or *Cnot7*$^{-/-}$ mice showing oligo-astheno-teratozoospermia. The *Ra175*$^{-/-}$ male mice were infertile due to the oligo-astheno-teratozoospermia. Some gene-targeted mice have been shown to be positive for oligo-astheno-teratozoospermia. Retinoic acid receptor-α (RARα) and retinoid X receptor-β (RXRβ) signals are essential for spermatogenesis. Male mice lacking RXRβ (*Rxrb*$^{-/-}$) and Cnot (*Cnot7*$^{-/-}$), a regulator of transcriptional function of RXRβ, are sterile due to an abnormal process of germ cell maturation that leads to oligo-astheno-teratozoospermia (17, 24). RA175 is at first isolated as the gene highly expressed during the differentiation of P19 EC cells induced by retinoic acid (9, 21, 29), making it possible to speculate that the deficiency of the RAR/RXR receptor signal leads to a lack of *Ra175* expression, resulting in a defect of spermatid-Sertoli cell junctions, which leads to abnormal spermiogenesis.

However, there is a remarkable morphological difference between *Ra175*$^{-/-}$ and *Rxrb*$^{-/-}$ or *Cnot7*$^{-/-}$ testes. In the *Rxrb*$^{-/-}$ and *Cnot7*$^{-/-}$ mutants, there is a progressive accumulation of lipids within the Sertoli cells and many terminal deoxynucleotidyltransferase-mediated dUTP-biotin nick end labeling-positive (apoptotic) cells in testes, and their seminiferous tubules contain degraded mature spermatids at

stages IX to XI as well as residual nuclear fragments at all the other stages (14, 20, 24). In contrast, a progressive accumulation of lipids and terminal deoxynucleotidyltransferase-mediated dUTP-biotin nick end labeling-positive cells was not detected (unpublished data), and elongated spermatids were almost not present in *Ra175*$^{-/-}$ testes. These phenotypic differences between *Ra175*$^{-/-}$ and *Rxrb*$^{-/-}$ or *Cnot7*$^{-/-}$ testes suggest that genes other than *Ra175* are also involved in the defect of spermiogenesis in *Rxrb*$^{-/-}$ or *Cnot7*$^{-/-}$ testes.

Oligo-astheno-teratozoospermia and defects in the elongating spermatid in the *Ra175*$^{-/-}$ mice. Light and electron microscopic analyses clearly showed that in *Ra175*$^{-/-}$ testes, germ cells normally differentiated into round spermatids but did not differentiate into mature elongated spermatids (Fig. 4 to 6); elongating spermatids (steps 9 to 12) were observed, but they failed to mature further. Thus, lack of mature elongated spermatid in *Ra175*$^{-/-}$ testes is one of the major causes for the oligo-astheno-teratozoospermia. In addition, the undifferentiated germ cells, including round spermatids and abnormally differentiated spermatids located at the adluminal surface, seem to exfoliate into the seminiferous tubular lumen, probably due to a weak association between the spermatids and Sertoli cells or denaturation of the abnormal and undifferentiated spermatids. Furthermore, Sertoli cells, similar to the residual bodies, may phagocytose the abnormally differentiated spermatids, which were not translocated to the adluminal surface. This possibility is supported by facts that the cell number of the remaining elongating spermatids decreased (asterisks in Fig. 5K and L) and that the phagocytosis of the abnormal elongated spermatids by Sertoli cells was frequently observed (Fig. 6D). Thus, deficiency of RA175 causes loss of the elongated and mature spermatids (steps 13 to 16) and the exfoliation and phagocytosis of the abnormal or undifferentiated elongated spermatids, leading to oligo-teratozoospermia. In addition, only a few spermatozoa found in the epididymis were immotile (Fig. 3). Owing to this, *Ra175*$^{-/-}$ male mice display oligo-atsheno-teratozoospermia and become sterile.

The phenotypic difference between *Ra175*$^{-/-}$ and *Nectin-2*$^{-/-}$ or *Jam-C*$^{-/-}$ mice. Until now, many genes of cell adhesion molecules in the immunoglobulin superfamily including nectin-2 and JAM-C have been disrupted (3, 4, 5, 12, 15, 23). Among them, *Jam-C*$^{-/-}$ and *Nectin-2*$^{-/-}$ male mice are infertile.

In *Jam-C*$^{-/-}$ testes, the differentiation of elongated spermatid is inhibited. Jam-C proteins, which have important functions in the assembly of tight junctions in endothelial and epithelial cells (1), are localized in most generations of spermatogenic cells, including round and elongated spermatids (15). Jam-C is confined to the junctional plaques in the heads of elongated spermatids and alters the adhesion structures, polarizing the localization of PAR-3 and anchoring spermatids to the Sertoli cell epithelium. Round spermatids in *Jam-C*$^{-/-}$ testes lack acrosomal structures and are defective in the polarization of the adhesion structures. This inhibits the differentiation of round spermatids into elongated spermatids (15).

In contrast with *Jam-C*$^{-/-}$ testes, the acrosomal structures of the round spermatids were uncompromised in *Ra175*$^{-/-}$ testes (Fig. 5 and 6). *Ra175*$^{-/-}$ germ cells can apparently and normally differentiate into the round spermatids with acrosomal structure. Furthermore, the level of the Jam-C was almost equal in *Ra175*$^{+/+}$ and *Ra175*$^{-/-}$ testes (unpublished data). Thus, lack of RA175 does not seem to affect the level of Jam-C, which provides the polarization of junctional plaque on the elongated spermatids.

However, Jam-C has a type II PDZ binding domain, which binds to polarizing proteins such as PAR-3 via PDZ domains (6, 7, 28). Since RA175 also has type II PDZ binding motifs at C terminals (2, 10), it may be possible that the lack of interaction between RA175 and proteins containing PDZ domains causes the change of the Jam-C distribution or localization on the elongated spermatid, providing the abnormal polarization or absence of junctional plaque, which induces the abnormal interaction between spermatid and Sertoli cells and results in the defect of the differentiation into the elongated spermatid. This possibility remains to be studied.

Nectin-2$^{-/-}$ male mice show a random disorganization of the spermatozoan head and midpiece due to overall disorganization of cytoskeletal structure, but they still possess motile spermatozoa (3, 23). The spermatid (steps 9 to 15) forms a Sertoli-spermatid junction via heterophilic interaction between nectin-2 and nectin-3 (23, 26). The association of the C termini of nectins and afadin, an actin-binding protein, is thought to participate in the assembly of actin filaments at the apical ectoplasmic specialization.

The following results suggest the distinct roles of the RA175 and nectins in the elongating spermatids. (i) Localization of RA175 on the elongated spermatid (steps 13 to 15) was restricted more distal to the head, near the tail (Fig. 5 and Table 1), whereas nectin-3 and nectin-2 are still restricted to around the head region of the elongated spermatid (26). (ii) There is the phenotypical difference between *Nectin-2*$^{-/-}$ and *Ra175*$^{-/-}$ mice. A deficiency in nectin-2 causes cytoskeletal disruption, resulting in the malformation of spermatids, but it does not induce the loss of the elongated spermatids or oligo-astheno-teratozoospermia (3, 23), while nectin-mediated spermatid-Sertoli cell junction and the cytoskeletal organization structure were normal; however, there was no maturation and no translocation of the elongated spermatid in *Ra175*$^{-/-}$ testes (unpublished data). Thus, RA175- and nectin-mediated cell junctions seem to have distinct roles in the distal portion and proximal portion in the spermatid-Sertoli cell junctions, respectively.

Possible roles of RA175-mediated cell junction in the distal portion of the elongated spermatids. Light and electron microscopical analyses (Fig. 5 and 6) clearly showed that in *Ra175*$^{-/-}$ testes, the elongating spermatids (steps 9 to 12) are defective and fail to proceed into the further maturation step, while *Ra175*$^{-/-}$ Sertoli cells seem to be normal; the lack of cell contact of the elongating spermatid with Sertoli cells in their invagination results in the incomplete differentiation, no maturation, and no translocation of the elongating spermatids.

Recently, in addition to TSLC1 and SynCAM, RA175 has been designated IGSF4A, SgIGSF, and Necl-2 (27, 30), which have been isolated from various tissues and cells, suggesting that RA175 has diverse biological functions in various tissues. However, both male and female *Ra175*$^{-/-}$ mice have not shown any altered behavior, including reproductive behavior and any incidence of tumor for almost 1 year. Furthermore, *Ra175*$^{-/-}$ mice had no overt developmental defects in tissues other than testes, suggesting that RA175-mediated cell junc-

tion is very essential for spermatogenesis in testes. Normally, the elongated spermatid is captured in the invagination of the Sertoli cells during displacement of the spermatid cytoplasm from the condensing nuclei during steps 13 to 15 (8). During these processes, the elongated spermatid receives the nutrition, hormones, and local factors required for maturation exclusively from the surrounding Sertoli cells. After this, it is translocated and released to the tubular lumen from the adluminal surface.

Defect of *IGSF4* (*TSLC1*), human orthologue of *Igsf4a* (*Ra175*), promotes the metastasis of lung carcinoma cells (18), suggesting that loss of RA175 makes the cells easily release from cell-to-cell interaction in some of the organs. It is likely that lack of RA175-mediated cell interaction makes the elongated spermatid and Sertoli cell adhesion unstable. Thus, RA175-mediated cell junction in the distal site retains the elongated spermatids in the invaginations of Sertoli cells until release as spermatozoa.

In conclusion, our results indicate that the RA175-based cell junction is necessary for anchoring the elongating spermatids to Sertoli cells. This specialization retains the elongated spermatid in the invagination of Sertoli cells during their complete differentiation and mediates the translocation of the elongated spermatids to the adluminal surface.

ACKNOWLEDGMENTS

We thank Shigeki Yuasa for valuable scientific discussion and Hisae Kikuchi for technical advice.

This work was supported in part by Grants-in-Aid from the Ministry of Education, Science and Culture of Japan and by Research Grant 14A-1 for Nervous and Mental Disorders and Research on Brain Science from the Ministry of Health and Welfare of Japan, the Human Science Foundation. E.F. and Y.K. are Research Fellows of the Japan Society for the Promotion of Science.

REFERENCES

1. **Aurrand-Lions, M., L. Duncan, C. Ballestrem, and B. A. Imhof.** 2001. JAM-2, a novel immunoglobulin superfamily molecule, expressed by endothelial and lymphatic cells. J. Biol. Chem. **276:**2733–2741.
2. **Biederer, T., Y. Sara, M. Mozhayeva, D. Atasoy, X. Liu, E. T. Kavalali, and T. C. Sudhof.** 2002. SynCAM, a synaptic adhesion molecule that drives synapse assembly. Science **297:**1525–1531.
3. **Bouchard, M. J., Y. Dong, B. M. McDermott, Jr., D. H. Lam, K. R. Brown, M. Shelanski, A. R. Bellve, and V. R. Racaniello.** 2000. Defects in nuclear and cytoskeletal morphology and mitochondrial localization in spermatozoa of mice lacking nectin-2, a component of cell-cell adherence junctions. Mol. Cell. Biol. **20:**2865–2873.
4. **Cremer, H., R. Lange, A. Christoph, M. Plomann, G. Vopper, J. Roes, R. Brown, S. Baldwin, P. Kraemer, S. Scheff, D. Barthels, K. Rajewsky, and W. Wille.** 1994. Inactivation of the N-CAM gene in mice results in size reduction of the olfactory bulb and deficits in spatial learning. Nature **367:**455–459.
5. **Dahme, M., U. Bartsch, R. Martini, B. Anliker, M. Schachner, and N. Mantei.** 1997. Disruption of the mouse L1 gene leads to malformations of the nervous system. Nat. Genet. **17:**346–349.
6. **Ebnet, K., A. Suzuki, S. Ohno, and D. Vestweber.** 2004. Junctional adhesion molecules (JAMs): more molecules with dual functions? J. Cell Sci. **117:**19–29.
7. **Ebnet, K., M. Aurrand-Lions, A. Kuhn, F. Kiefer, S. Butz, K. Zander, M. K. Meyer zu Brickwedde, A. Suzuki, B. A. Imhof, and D. Vestweber.** 2003. The junctional adhesion molecule (JAM) family members JAM-2 and JAM-3 associate with the cell polarity protein PAR-3: a possible role for JAMs in endothelial cell polarity. J. Cell Sci. **116:**3879–3891.
8. **Fawcett, D. W.** 1986. A textbook of histology, p. 796–850. *In* W. Bloom and D. W. Fawcett (ed.), Male reproductive system, Saunders Company, Philadelphia, Pa.
9. **Fujita, E., A. Soyama, K. Urase, T. Mukasa, and T. Momoi.** 1998. RA175, which is expressed during the neuronal differentiation of P19 EC cells, temporally expressed during neurogenesis of mouse embryos. Neurosci. Res. **22:**283.
10. **Fujita, E., A. Soyama, and T. Momoi.** 2003. RA175, which is the mouse orthologue of TSLC1, a tumor suppressor gene in human cancer, is a cell adhesion molecule. Exp. Cell. Res. **287:**57–66.
11. **Fujita, E., K. Urase, A. Soyama, Y. Kouroku, and T. Momoi.** 2005. Distribution of RA175/TSLC1/SynCAM, a member of the immunoglobulin superfamily, in the developing nervous system. Dev. Brain Res. **154:**199–209.
12. **Fukamauchi, F., O. Aihara, Y. J. Wang, K. Akasaka, Y. Takeda, M. Horie, H. Kawano, K. Sudo, M. Asano, K. Watanabe, and Y. Iwakura.** 2001. TAG-1-deficient mice have marked elevation of adenosine A1 receptors in the hippocampus. Biochem. Biophys. Res. Commun. **281:**220–226.
13. **Fukami, T., H. Satoh, E. Fujita, T. Maruyama, H. Fukuhara, M. Kuramochi, S. Takamoto, T. Momoi, and Y. Murakami.** 2002. Identification of the Tslc1 gene, a mouse orthologue of the human tumor suppressor TSLC1 gene. Gene **295:**7–12.
14. **Gehin, M., M. Mark, C. Dennefeld, A. Dierich, H. Gronemeyer, and P. Chambon.** 2002. The function of TIF2/GRIP1 in mouse reproduction is distinct from those of SRC-1 and p/CIP. Mol. Cell. Biol. **22:**5923–5937.
15. **Gliki, G., K. Ebnet, M. Aurrand-Lions, B. A. Imhof, and R. H. Adams.** 2004. Spermatid differentiation requires the assembly of a cell polarity complex downstream of junctional adhesion molecule-C. Nature **431:**320–324.
16. **Goossens, S., and F. van Roy.** 2005. Cadherin-mediated cell-cell adhesion in the testis. Front. Biosci. **10:**398–419.
17. **Kastner, P., M. Mark, M. Leid, A. Gansmuller, W. Chin, J. M. Grondona, D. Decimo, W. Krezel, A. Dierich, and P. Chambon.** 1996. Abnormal spermatogenesis in RXR beta mutant mice. Genes Dev. **10:**80–92.
18. **Kuramochi, M., H. Fukuhara, T. Nobukuni, T. Kanbe, T. Maruyama, H. P. Ghosh, M. Pletcher, M. Isomura, M. Onizuka, T. Kitamura, T. Sekiya, R. H. Reeves, and Y. Murakami.** 2001. TSLC1 is a tumor-suppressor gene in human non-small-cell lung cancer. Nat. Genet. **27:**427–430.
19. **Lui, W. Y., D. Mruk, W. M. Lee, and C. Y. Cheng.** 2002. Sertoli cell tight junction dynamics: their regulation during spermatogenesis. Biol. Reprod. **68:**1087–1097.
20. **Mascrez, B., N. B. Ghyselinck, M. Watanabe, J. S. Annicotte, P. Chambon, J. Auwerx, and M. Mark.** 2004. Ligand-dependent contribution of RXR beta to cholesterol homeostasis in Sertoli cells. EMBO Rep. **5:**285–290.
21. **McBurney, M. W., E. M. Jones-Villeneuve, M. K. Edwards, and P. J. Anderson.** 1982. Control of muscle and neuronal differentiation in a cultured embryonal carcinoma cell line. Nature **299:**165–167.
22. **Mruk, D. D., and C. Y. Cheng.** 2004. Cell-cell interactions at the ectoplasmic specialization in the testis. Trends Endocrinol. Metab. **15:**439–447.
23. **Mueller, S., T. A. Rosenquist, Y. Takai, R. A. Bronson, and E. Wimmer.** 2003. Loss of nectin-2 at Sertoli-spermatid junctions leads to male infertility and correlates with severe spermatozoan head and midpiece malformation, impaired binding to the zona pellucida, and oocyte penetration. Biol. Reprod. **69:**1330–1340.
24. **Nakamura, T., R. Yao, T. Ogawa, T. Suzuki, C. Ito, N. Tsunekawa, K. Inoue, R. Ajima, T. Miyasaka, Y. Yoshida, A. Ogura, K. Toshimori, T. Noce, T. Yamamoto, and T. Noda.** 2004. Oligo-astheno-teratozoospermia in mice lacking Cnot7, a regulator of retinoid X receptor beta. Nat. Genet. **36:**528–533.
25. **Ozaki, H., Y. Watanabe, K. Takahashi, K. Kitamura, A. Tanaka, K. Urase, T. Momoi, K. Sudo, J. Sakagami, M. Asano, Y. Iwakura, and K. Kawakami.** 2001. Six 4, a putative myogenin gene regulator, is not essential for mouse embryonal development. Mol. Cell. Biol. **21:**3343–3350.
26. **Ozaki-Kuroda, K., H. Nakanishi, H. Ohta, H. Tanaka, H. Kurihara, S. Mueller, K. Irie, W. Ikeda, T. Sakai, E. Wimmer, Y. Nishimune, and Y. Takai.** 2002. Nectin couples cell-cell adhesion and the actin scaffold at heterotypic testicular junctions. Curr. Biol. **12:**1145–1150.
27. **Shingai, T., W. Ikeda, S. Kakunaga, K. Morimoto, K. Takekuni, S. Itoh, K. Satoh, M. Takeuchi, T. Imai, M. Monden, and Y. Takai.** 2003. Implications of nectin-like molecule-2/IGSF4/RA175/SgIGSF/TSLC1/SynCAM1 in cell-cell adhesion and transmembrane protein localization in epithelial cells. J. Biol. Chem. **278:**35421–35427.
28. **Suzuki, A., C. Ishiyama, K. Hashiba, M. Shimizu, K. Ebnet, and S. Ohno.** 2002. aPKC kinase activity is required for the asymmetric differentiation of the premature junctional complex during epithelial cell polarization. J. Cell Sci. **115:**3565–3573.
29. **Urase, K., A. Soyama, E. Fujita, and T. Momoi.** 2001. Expression of RA175 mRNA, a new member of immunoglobulin super family, in developing mouse brain. NeuroReport **12:**3217–3221.
30. **Watabe, K., A. Ito, Y. I. Koma, and Y. Kitamura.** 2003. IGSF4: a new intercellular adhesion molecule that is called by three names, TSLC1, SgIGSF and SynCAM, by virtue of its diverse function. Histol. Histopathol. **18:**1321–1329.
31. **Wilkinson, D. G.** 1992. Whole mount in situ hybridization of vertebrate embryos, p. 75–83. *In* D. G. Wilkinson (ed.), In situ hybridization: a practical approach, Oxford IRL Press, New York, N.Y.